Concept of SPARC4: A Simultaneous Polarimeter and Rapid Camera in 4 Bands

Claudia V. Rodrigues[a], Keith Taylor[b], Francisco J. Jablonski[a], Marcelo Assafin[c], Alex Carciofi[d], Deonisio Cieslinski[a], Joaquim E. R. Costa[a], Ruben Dominguez[e], Tania P. Dominici[f], Gabriel A. P. Franco[g], Damien Jones[h] Antonio Kanaan[i], René Laporte[a], Antonio Mario Magalhães[d], André Milone[a], José A. Neri[a],Antonio Pereyra [j], Luiz A. Reitano[a], Karleyne M. G. Silva[a], Cesar Strauss[a]

[a]Instituto Nacional de Pesquisas Espaciais, Brazil;
[b]Instruments4, United States of America;
[c]Observatório do Valongo, Brazil;
[d]Universidade de São Paulo, Brazil;
[e]University of Arizona, United States of America;
[f] Laboratório Nacional de Astrofísica, Brazil;
[g]Universidade Federal de Minas Gerais, Brazil;
[h]Prime Optics, Australia;
[i]Universidade Federal de Santa Catarina, Brazil;
[j]Instituto de Astrofísica de Canarias, Spain

ABSTRACT

We present a summary of the concept design report of a new astronomical instrument: SPARC4, Simultaneous Polarimeter and Rapid Camera in 4 bands. SPARC4 will provide photometry and polarimetry in four optical broad bands (griz SDSS) simultaneously. This is achieved by the use of dichroic beam splitters. The square field of view is around 5.6 arcmin on a side. SPARC4 time resolution is sub-second for photometry and somewhat longer for polarimetry. This is provided by the use of fast EMCCDs. The main motivation for building SPARC4 is to explore astrophysical objects which exhibit fast temporal variability in flux and polarization. The instrument will be installed at the 1.6-m telescope of the Observatório do Pico dos Dias (Brazil).

Keywords: SPARC4, OPD, astronomical instrumentation, optical instrumentation, photometers, imaging polarimetry, astrometry

1. MANUSCRIPT ORGANIZATION

This manuscript describes the concept study of the instrument SPARC4: Simultaneous Polarimeter and Rapid Camera in 4 bands. It is organized as follows. Section 2 describes the motivation to build SPARC4 and similar instruments for comparison. The science cases are presented in Sec. 3. The SPARC4 concept is summarized in Sec. 4. The simulated instrument's photometric performance is shown in Sec. 5. Finally, we present the status of the project and the expected future developments (Sec. 6).

2. RATIONALE

SPARC4 will be an instrument to perform simultaneous imaging in four broad bands with sub-second time resolution. Additionally, it will have polarimetric capabilities. We propose to build SPARC4 and install it at Observatório do Pico dos Dias (OPD), in Brazil, to improve the observatory efficiency in its traditional research areas. SPARC4 is conceived mainly, but not only, to explore variability in the time domain with differential

Further author information: (Send correspondence to C.V.R.)
C.V.R.: E-mail: claudiavilega@gmail.com, Telephone: +55 (12) 3208-7210

Ground-based and Airborne Instrumentation for Astronomy IV, edited by Ian S. McLean, Suzanne K. Ramsay, Hideki Takami, Proc. of SPIE Vol. 8446, 844626 · © 2012 SPIE · CCC code: 0277-786X/12/$18 · doi: 10.1117/12.924976

techniques for gathering data. Specifically, SPARC4 can be used to perform photometry, polarimetry, and astrometry. These differential techniques allow an optimized use of the OPD site given its average atmospheric conditions and an increase in the scientific production of OPD as measured by refereed articles, theses, and dissertations. SPARC4 is anticipated to be a heavily demanded instrument among the present options at this observatory, which contributes a large fraction of the Brazilian optical observational astronomy productivity.

SPARC4 is a four band version of IAGPOL,[1] a polarimeter currently in use at OPD. In a broad context, it is useful to compare SPARC4 with similar instruments around the world. The most relevant are listed below.

- TurPol[2,3] is a simultaneous five-color (UBVRI) polarimeter that uses photomultipliers as detectors. The color selection is done using dichroic beam splitters. It cannot perform polarimetry and differential photometry simultaneously. It is available on the 2.56-m Nordic Optical Telescope (NOT) on the La Palma astronomical site.
- ULTRACAM[4] is an optical three-band imager with an impressive frame rate of up to 500 Hz achieved using customized readout modes. It is not a polarimeter.
- GROND[5] is a 7-channel (4 optical and 3 near-infrared) imager and does not have polarimetric capability. It was commissioned at the 2.2-m Max Planck Institute telescope at ESO in April 2007.
- HIPPO[6] is a two-channel optical imager with polarimetric capability. The bands are selected by a chopping filter wheel and the detectors are photomultiplier tubes. It is used at the 1.9-m telescope of the South African Astronomical Observatory (SAAO).
- RINGO2[7] is a polarimeter installed at the 2.0-m Liverpool Telescope, a fully robotic telescope. It uses an electron multiplying (EM) CCD and works in one band that approximately covers the V and R ranges, optimized for Gamma Ray Bursts (GRB) studies.
- ZIMPOL's[8] main science case is exoplanets. The instrument's main characteristics is the high polarimetric sensitivity, of 10^{-5}. It will be installed at the VLT/ESO telescope as part of the SPHERE instrument, a stellar coronagraph using an adaptive optics system.

To our knowledge, SPARC4 is unique by combining good time resolution, polarimetry, and four optical broad bands simultaneity.

3. SCIENCE CASES

In this section, we outline some science cases that motivated us to build SPARC4. Our examples derive from results obtained at OPD by our team, but, of course, there are other science cases which will benefit from an instrument like SPARC4.

3.1 Interacting binaries

Interacting binaries include objects as cataclysmic variables (CV), X-ray binaries, and symbiotic systems. Their common denominator is mass transfer between the components producing conspicuous time variability spanning scales from seconds to years. The multi-band photometry and polarimetry put hard constraints on the physical and geometrical properties of interacting binaries. An example is the determination of the properties of the accretion columns in magnetic CVs.[9,10] The sub-second time resolution of SPARC4 is adequate to study rapid oscillations and flickering arising in the mass transfer structures.[11] Eclipse mapping, ellipsoidal variations, and reflection effects are other examples of photometric techniques that can bring detailed information of stars and accretion structures on interacting binaries.

3.2 Pulsating stars

The oscillations of pulsating stars occur simultaneously in many modes, something which puts strong constraints on the theoretical models of their internal structure. One particularly interesting case of pulsating stars is pulsating white dwarfs. Their many modes can be difficult to detect owing to their low amplitude (as small as few millimagnitudes), but also because they are very closely spaced in frequency. In order to resolve all pulsation modes, and therefore extract useful information from the observations, continuous data are needed for around two weeks extent at a sampling rate of 10 seconds. The Brazilian community has had a leading role in the Whole Earth Telescope (WET), a loosely assembled group who has made important contributions in the area of white dwarfs seismology.[12,13] Other pulsating stars are δ Scuti stars, rapidly oscillating Ap stars, Cepheids, and Be stars.

3.3 Exoplanets

The study of exoplanets is certainly an important area of research nowadays. The Brazilian astronomical community shows also a growing interest in the field of exoplanets.[14–16] For those cases of exoplanets where transits can be observed, an instrument like SPARC4 is very competitive since it can provide simultaneous differential photometry in four bands. Multicolor observations and good time resolution are key for deriving parameters like the limb-darkening coefficient of the parent star.[17,18] The exoplanet research can also be performed using polarimetric techniques.[14] This kind of observations has received much less attention than photometry, and this is mostly due to the scarceness of suitable instruments. SPARC4 will provide new opportunities in this front. Another topic related to exoplanets where the instrument will set new standards is the observation of anomalies in the gravitational lensing amplification pattern caused by the alignment of observer-(mass)lens-source.[19–22] The insertion of the new instrument in worldwide collaborations like μFun (http://www.astronomy.ohio-state.edu/ microfun/) is very important to sort out false positives.

3.4 Circumstellar envelopes

Studies of circumstellar material in different kinds of objects - as young stellar objects, Be stars, and protoplanetary nebulae - could also see the benefits of multicolor polarimetric observations provided by SPARC4. Generally speaking, polarimetry constrains the geometry of the circumstellar material and, complementarily, the spectral flux and polarization dependence constrains the optical properties of the matter, independently of being gas or dust particles.[23–25]

The circumstellar material distribution can also be time variable. Long-term photometric, polarimetric, and spectroscopic monitoring of several bright Be stars has been conducted at OPD. The goal is to detect, monitor and characterize the variations of the target stars in several time scales, from hours/days to months/years.[26] Those observations are part of a broader, multi-technique observing campaign involving the AMBER interferometer at VLT/ESO, the FEROS spectrograph and more recently the APEX/ESO radio telescope. SPARC4 will have a large impact in this kind of study. Today, at OPD, it is possible to do BVRI polarimetry of about 10-12 target stars per night, because each filter must be cycled sequentially. With the new instrument, the productivity can be increased by at least a factor of four.

3.5 Star forming regions

The role of magnetic fields in star formation is a longstanding problem in astrophysics. Specifically, the importance of the interstellar magnetic field (ISMF) in supporting molecular clouds is controversial.[27,28] As the position angle of the optical interstellar polarization traces the ISMF in the plane of sky, it is possible to map and quantify the ISM alignment using polarimetry.[29–31] Some recent results obtained at OPD on ISMF are: ISMF structure on the Pipe Nebula;[32,33] correlation between the ISMF direction and the symmetry axis in Herbig Ae/Be stars;[34] and space distribution of the ISMF around Herbig-Haro objects.[35] Additionally, the spectral dependence of the interstellar polarization can be used to study the size, composition, and alignment of the interstellar grains.[36]

3.6 Blazars

The emission from blazars is predominantly non-thermal in origin and highly variable, in scales as short as a few minutes.[37] There is evidence that most of the variability is related to close alignment of the relativistic beamed emission with the line of sight. Polarimetric observations indicate that the brightness variations cannot be explained by an unique homogeneous source, rather, by a superposition of different components. A comparison between total flux density and the associated polarized fraction may indicate whether the observed variations are produced in the beamed source. Simultaneous multi-band observations are crucial to the study of the spectral slopes and time lags at distinct frequencies. Polarimetric measurements are also important for the identification of the magnetic field structure along the relativistic jet.[38] An instrument with capabilities of providing total flux, polarized fractions, and simultaneous measurements in four bands has the potential of producing a complete, unprecedented set of data for the investigation of the nature of the variability source in blazars. Recently, polarimetric observations taken at OPD simultaneously with a gamma-ray campaign of a few days (H.E.S.S. collaboration, http://www.mpi-hd.mpg.de/hfm/HESS/) allowed to propose a multi-zone model to explain the variability in time scales of hours and days and the complex relation observed between total and polarized flux.[39] The analysis of spectral variations in optical and its relation with higher energy variations was limited by the lack of simultaneity in the observations taken in only three bands. An instrument like SPARC4 will give us the opportunity to obtain really simultaneous observations with a broad spectral coverage in the optical; both important aspects to better constrain the proposed models.

3.7 Solar system studies

Time variability of solar systems objects can occur in events such as mutual phenomena - occultations and eclipses among binary asteroids and planetary satellites - and stellar occultations by planets, its satellites, asteroids, and particularly transneptunian objects. The determination of the size, the albedo and the atmosphere limits for Eris is a recent example of an international observational campaign in this area.[40] In case of stellar occultations of bodies with atmosphere, simultaneous multi-band observations could help in detecting aerosols and atmospheric structures (including hazes) by the presence of coherent flickering in the light curves of different colors. Dynamical studies of solar systems bodies can also be carried out with an instrument like SPARC4.[41–43]

3.8 Stellar populations and open clusters

Taking the advantage of simultaneously measuring SDSS magnitudes over a fairly wide field of view (FoV), SPARC4 will allow us to undertake interesting surveys of stars in the Sun's neighborhood. Furthermore, the SDSS colors have been exhaustively tested and calibrated to measure stellar parameters with great confidence.[44] The motivation is to generate a census of nearby stars, especially covering the thin disc through a homogeneous compilation of good quality data. The close solar neighborhood has been partially neglected by recent Galactic surveys.[45,46]

Open clusters have long been recognized as important objects to investigate aspects of Galactic structure such as the chemical abundance gradients in the disk. Imaging is an essential tool to the determination of their fundamental parameters. SPARC4 can be used to characterize an open cluster, since it is possible to statistically measure the metallicity, temperature and gravity of the member stars by using the griz SDSS colors. The derived individual stellar parameters can be adopted to make more consistent the direct stars-isochrone comparisons on the theoretical H-R diagram $\log(L/L_{\odot})$ vs. $\log(T_{eff})$ to derive the cluster's age and chemistry.

Optical imaging polarimetry of open clusters can provide the length scale of the uniform component of the ISMF.[47]

4. CONCEPT OVERVIEW

The optical sketch of SPARC4 is depicted in Fig. 1. The instrument can be summarized as a set of four CCD cameras working simultaneously in the griz SDSS broad bands.[48] The white beam is split by three dichroic mirrors. Before this splitting, the white beam may optionally pass through a polarimetric unit. Below we describe briefly the main units of SPARC4. Some parts of the concept study are detailed in Secs. 4.1, 4.2, and 4.3. The main characteristics of SPARC4 are presented in Table 1.

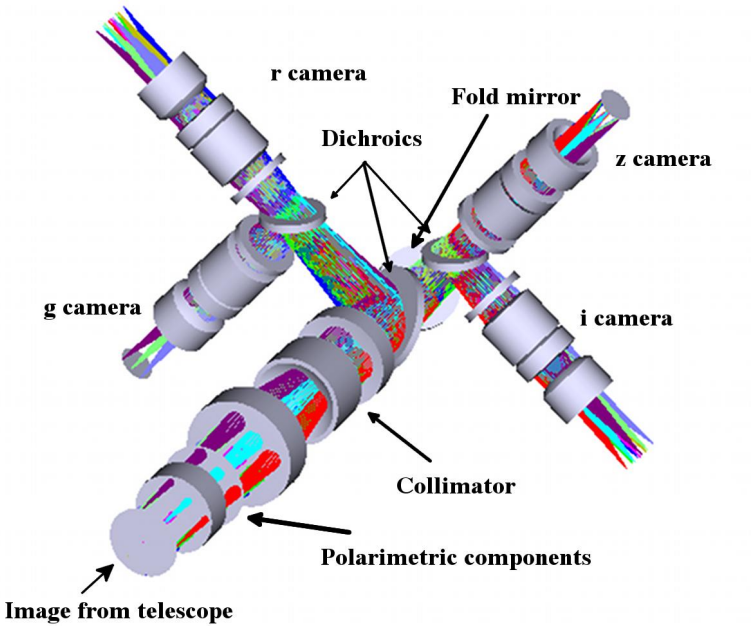

Figure 1. SPARC4 optical design concept.

From the telescope, light firstly encounters an *autoguider* (AG). The AG field of view (FoV) is ≈3 arcmin on a side which can be positioned anywhere within an annular region surrounding the main FoV. The inclusion of an autofocusing mechanism based on a 2×2 array of Shack-Hartmann lenslets is being studied. The present choice for the autoguider detector is the Andor Luca(R) camera. It employs a thermoelectrical cooled EMCCD, having 1000×1000, 8 μm pixels.

After the AG, light passes through the *polarimetric unit*. This has a wheel with optical elements necessary to calibrate the instrumental polarization and the polarimetric efficiency. After the wheel, light encounters a retarder waveplate and an analyzer. The user can select from two retarders: $\lambda/2$ or $\lambda/4$. They allow linear or linear-and-circular polarimetry. The analyzer is a Savart plate. The whole polarimetric unit can be taken out of the beam to allow standard photometry.

The white beam is then *collimated*. The split in four colors is performed by three *dichroic mirrors*. *Filters* will be used to finetune the SPARC4 photometric system to provide responses as similar as possible to the griz SDSS bands. The natural focal ratio of the Cassegrain focus is f/10, which is reduced to f/5 in the SPARC4 *camera*.

Finally, the light in each band is *detected* by an Andor Ixon(EM)-888 camera, based on the e2v CCD201-20 sensor. It has 1024×1024, 13 μm pixels. The electron multiplication of this camera makes it very sensitive and adequate for photometry of faint objects, especially when time-domain information is important. Recent improvements to this camera lead to a reduction of the near infrared fringing and an enhancement in the quantum efficiency (EX2 technology). The Ixon(EM)-888 camera has a fast readout: up to 10 MHz. The readout noise is intrinsically low, 6 e- using the conventional amplifier, and can be dramatically reduced in the EM mode.

SPARC4 will be delivered with control, acquisition, and reduction pipeline softwares. A quick look (photometric and polarimetric) reduction to guide decisions during the night is also planned, as well as an integration time calculator (ITC).

All systems and softwares should be properly documented to facilitate maintenance and usage.

We have already an estimate for the SPARC4 cost. It includes the design, components, and fabrication costs.

Table 1. Main characteristics of SPARC4 and telescope.

Telescope f#	f/10
Telescope aperture	1.6 m
Final f#	f/5
Main detectors	Andor Ixon(EM)-888
Pixels	1024×1024
Pixel size	13 μm $\times$ 13 μm
Field of view	5.6 arcmin $\times$ 5.6 arcmin
Final platescale	0.0254 arcsec/μm 0.35 arcsec/pixel
Bands	griz SDSS
Weight	175 kg
Modes of operation	photometry polarimetry of program stars polarimetric calibration
Time resolution	$<$ 1 s (photometric mode - entire detector - fast readout)
Magnitudes for photometric SNR = 10	19 mag, for t_{exp} = 1 s 21 mag, for t_{exp} = 10 s 21.8 mag, for t_{exp} = 300 s

4.1 Optical Layout

This section presents an overview of the SPARC4 optical design including the polarimetric elements, the collimator, the camera, and the filters as well as a ghost and a tolerance analysis. We begin by discussing the need for a compensator to bring to the same focus the instrument in the different modes of operation is discussed.

The beam encounters different optical components in the polarimetric unit according to each of the instrument modes of operation: photometry, polarimetric calibration, or standard polarimetry. An element of fused silica with the appropriate optical thickness can be used to compensate the different optical paths in each mode. This will bring the instrument to the same focus in all modes and also compensate spherical aberration caused by the plane parallel components. The optical study shows that all modes can be compensated including a single fused silica slab of 19.8 mm thickness, being half of the width of the thickest compensator.

The collimator is composed of three all spherical cemented doublets. The design provides the best collimation at the beamsplitters' positions. The 80% encircled energy diameter (EED80) broadband performance is approximately 12 μm and increases to a maximum of 13 μm at the extremes optical paths.

The cameras are composed of 3 components: two doublets and a singlet. It is useful to have two types of cameras depending on the wavelength: red (550–1000 nm) and blue (380–550nm) in order to partially correct collimator aberrations. The EED80 is between 8 and 9.5 μm.

The optical quality of the entire system is illustrated by spot diagrams and graphs of the fraction of encircled energy (Figs. 2 and 3, respectively). The configurations 1, 2, and 3 represent zero, nominal average, and maximum fused silica equivalent thickness in the polarimetric unit, respectively. The worst EED80 is around 10 μm. The optical design meets the requirements of having EED80 with the spots within one pixel.

The ghost analysis was performed considering 2-reflection images and pupil ghosts. The actions to minimize ghosts are:

- to tilt by about 5 degrees the filter in the collimated space before camera;

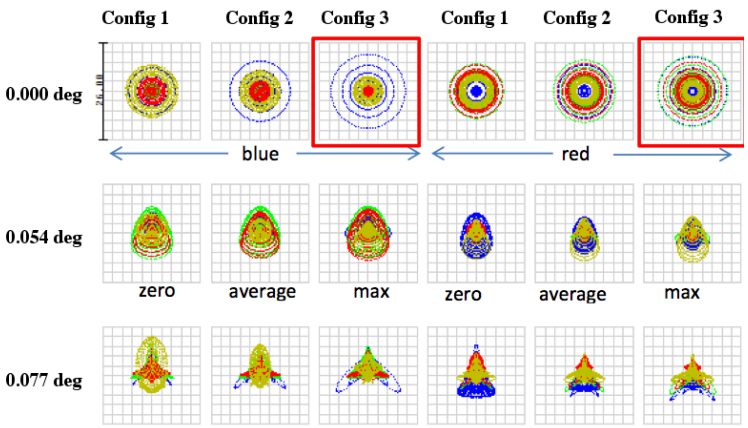

Figure 2. Spot diagram of SPARC4 for the blue and red cameras including the polarimetric elements. The spots are shown for three positions on the field (0.0, 3.24, and 4.62 arcmin, from top to bottom) and three fused silica equivalent optical thickness in the polarimetric unit (in horizontal direction).

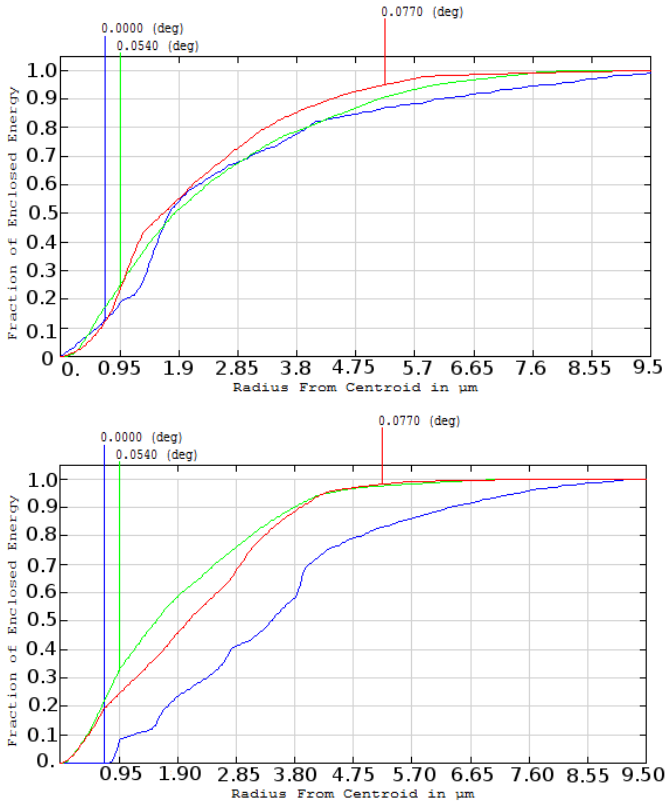

Figure 3. (Top) 80% Encircled Energy Radius (EER80) for the blue camera. (Bottom) EER80 for the red camera.

- to deploy the polarimetric unit as close as possible to the collimator;
- to use good broadband anti-reflection coatings, especially in the polarimetric and collimator components.

4.2 Mechanical design

The preliminary SPARC4 mechanical design is shown in Fig. 4. It includes: the structure; the autoguider box; the polarimetric calibrating wheel (Fig. 5, left); the positioning and rotation of the retarders (Fig. 5, right); the

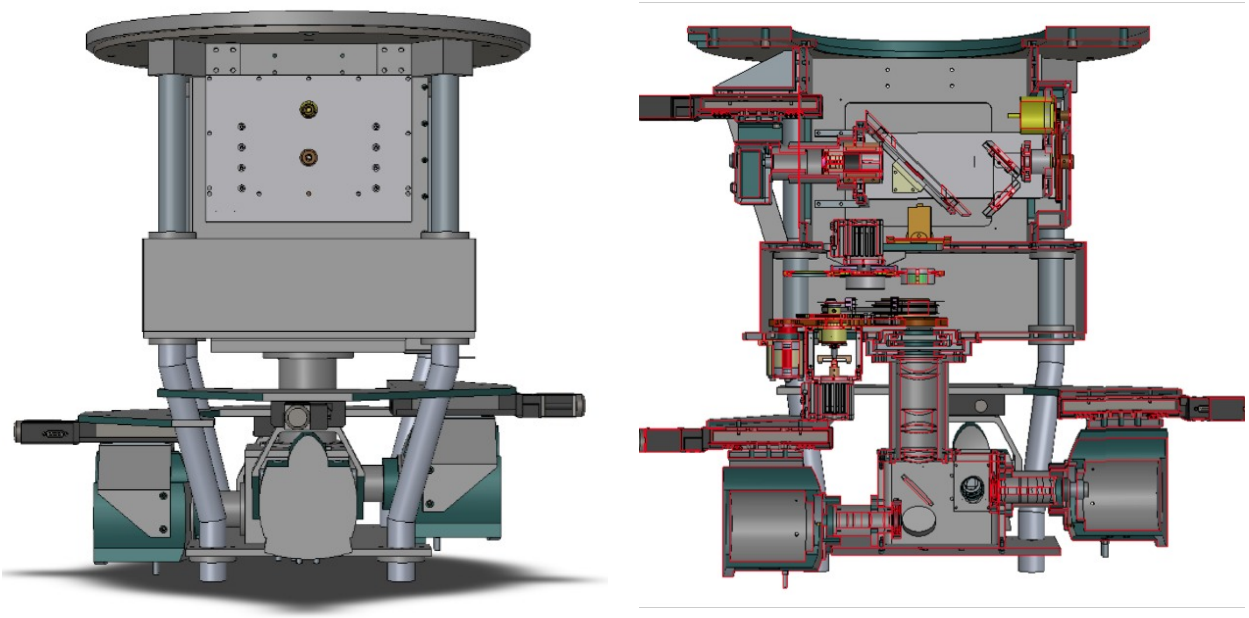

Figure 4. (Left) External view of the SPARC4 mechanical structure. (Right) Internal view of the structure.

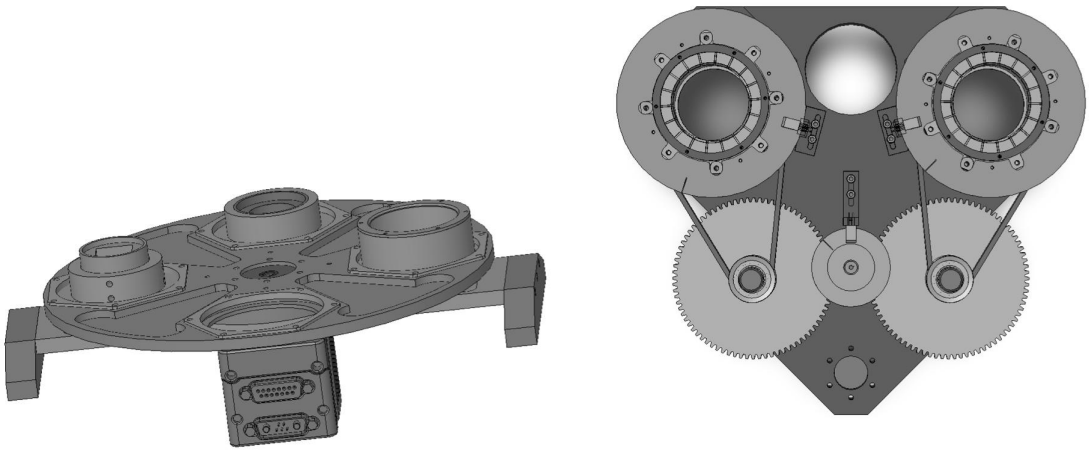

Figure 5. Detailed view of some mechanical parts. (Left) Calibrating wheel. (Right) Retarders support.

positioning of the analyzer; the collimator; the dichroics; filter slides; cameras; and detectors.

The total length of the instrument, from telescope flange to detectors, is 813.4 mm. The mechanical requirement for the telescope load is: 250 kg at 0.305 m. This translates into a torque of 76.25 kg.m, while for our instrument we have 70 kg.m, in the comfort zone for normal operations. The finite element analysis (FEA) indicates small but nevertheless significant flexures. In the preliminary design phase, we plan to study alternative structures. An example is a structure based on (filled or open) boxes, instead of bars. This design can be easier to fabricate and assemble.

The location of the shutter has not been decided yet, as well as whether we will adopt an off-the-shelf solution or design one.

4.3 Control system

SPARC4 has a relatively large number of moving parts. Most of them have necessarily to be motorized. Below we enumerate the planned movements.

Cameras position: We plan manually move the four scientific cameras. This movement will allow us to fine-tune the camera position in the commissioning phase of the instrument. Presently, it is not clear whether the guider camera has to be motorized. This answer will be delivered by the study of an eventual auto-focus mechanism.

Autoguider mirror: A motorized movement is certainly necessary to patrol the peripheral FoV.

Positioning of the polarimetric calibrating wheel: This movement will be actuated many times during an observing night, so a motorized movement is required.

Choice of the waveplate (WP): $\lambda/2$, $\lambda/4$, or off. This can be a manual movement, because we foresee most users will be limited to only one mode during a night.

WP rotation: This movement is the heart of the polarimetric mode; it should be motorized.

Positioning the analyzer (on/off): As for the choice of the WP, this can be a manual movement, since we expected most users will use only one position during a night.

Filters: The filter slides in each arm will be manually operated.

The final decision about remote control of movements will be done based on the costs and operational requirements, as we go to a more detailed design of the control system. Whether a movement is manual or motorized, we would like to have all positions registered by encoders and noted on the control screen and added to the image header, allowing the system (and user) to keep track of the instrument configuration.

A preliminary solution to control the moving parts of SPARC4 was proposed by the Brazilian company Solunia. This solution is based on industrial stepper motors and controllers (CPU/PLC - programmable logic controllers) from Beckhoff (Germany) and 24 bit SSI absolute encoders from IFM (Germany). Solunia has provided an estimate of the costs of the SPARC4 control system including: hardware, system integration, control panel, software, documentation, and training.

5. SIMULATION OF THE SPARC4 PHOTOMETRIC PERFORMANCE

The photometric system was simulated to include: sky transparence; optical efficiencies including the dichroics and filters; and the detector response. The study allowed us to define the split wavelength of the dichroics, the importance of complementary filters (Schott glasses) to reproduce the SDSS photometric system, and the sensor vendor options regarding the coating that determines the detailed shape of the quantum efficiency (QE). The filters used in the study follow the SDSS recipe.[48]

There are two relevant options for coating for the Andor iXon3 888 sensors: standard anti-reflection (A/R) coating and EX2 coating - a new technology based on dual coating that improves the blue response. We searched for the best combination of cut-off wavelengths of the dichroics and coatings to reproduce the SDSS system using filters. The best results are obtained using the cut-off wavelengths presented in Table 2, the standard A/R coating in the riz bands and the EX2 coating in the g band. We will call this solution Mode A. The pivotal wavelengths, λ_p, and widths, FWHM, of Mode A are presented in Table 3. This table also shows λ_p and FWHM of the SDSS bands. In mode A, the expected SPARC4 signal-to-noise ratio (SNR) is illustrated by Fig. 6.

We foresee that some SPARC4 users may be interested in maximizing the count rate at the expense of a close match to the SDSS system. These users can opt for using no filters at all. This will be called Mode B. Table 3 shows λ_p and FWHM of mode B. The agreement with the SDSS pivotal wavelengths is not too discouraging, even for Mode B. Moreover, the counts are 20% (r and i bands) to 100% (g band) larger than in Mode A, resulting in a larger SNR.

Table 2. Split wavelengths of the dichroics to a good agreement with the SDSS photometric system (see text).

Dichroic	Split wavelength (nm)
gr	535
ri	667
iz	827

Table 3. Pivotal wavelengths and widths of the SDSS system and Modes A and B of SPARC4.

Band	SDSS		Mode A		Mode B	
	λ_p (nm)	FWHM (nm)	λ_p (nm)	FWHM (nm)	λ_p (nm)	FWHM (nm)
g	470.3	92.8	473.0	92.7	457.3	246.1
r	617.6	81.2	613.4	89.8	603.6	113.1
i	749.0	89.4	758.5	89.7	747.4	111.3
z	894.7	118.3	889.9	116.3	894.7	135.3

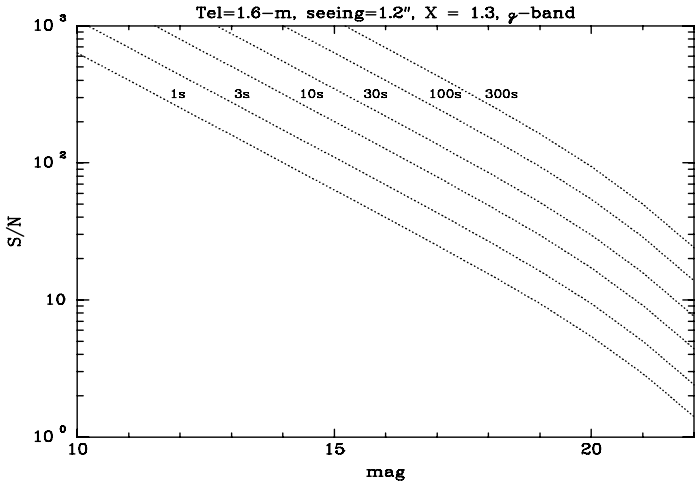

Figure 6. Modeled signal-to-noise ratio for SPARC4 in the g band for different exposure times using filters (Mode A, see text).

It is also useful to study the transformation of SPARC4 to SDSS magnitudes. Figure 7 shows the modeled differences between SPARC4 and SDSS magnitudes as function of the SDSS (g-r) color using as input the spectra of Gunn & Striker.[49] They indicate a well behaved linear relation between the two systems.

6. CURRENT STATUS AND FUTURE DEVELOPMENTS

The Conceptual Study proposes solutions to all SPARC4 sub-systems and shows that the project is feasible. The estimated total cost of the instrument is US$ 650k: around one third of this is due to the detectors.

The Conceptual Design Review will occur by mid-2012. We expect to start the Preliminary Design Phase in the second semester of 2012.

ACKNOWLEDGMENTS

This project is partially funded by Fapesp (Proc. 2010/01584-8). AMM is supported by Fapesp grant no. 2010/19694-4. GAPF is partially supported by FAPEMIG. CNPq partially supports AK, AMM, CVR (308005/2009-0), and GAPF.

REFERENCES

[1] Magalhães, A. M., Rodrigues, C. V., Margoniner, V. E., Pereyra, A., and Heathcote, S., "High Precision CCD Imaging Polarimetry," in [*Polarimetry of the Interstellar Medium*], Roberge, W. G. and Whittet, D. C. B., eds., *ASPCS* **97**, 118 (1996).

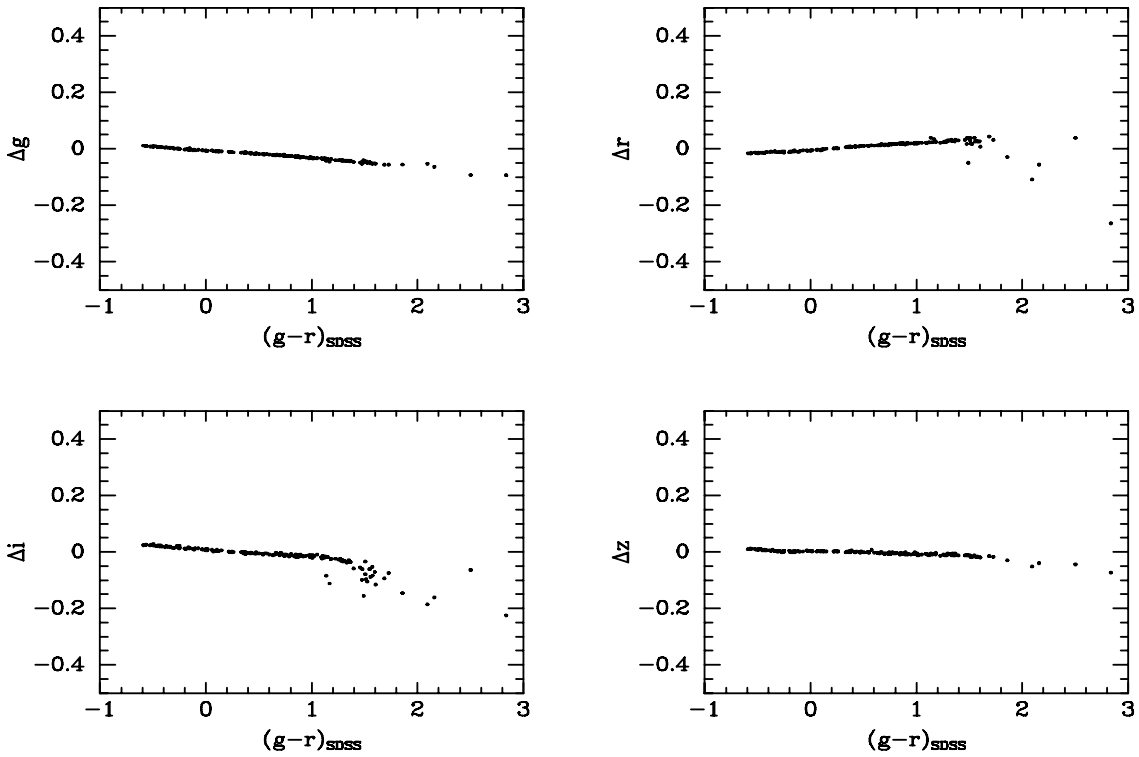

Figure 7. Simulated differences between SPARC4 and SDSS magnitudes as a function of SDSS colors.

[2] Korhonen, T., Piirola, V., and Reiz, A., "Polarization measurements at La Silla," *The Messenger* **38**, 20–24 (1984).

[3] Piirola, V., "Simultaneous five-colour (UBVRI) photopolarimeter," in [*Polarized Radiation of Circumstellar Origin*], Coyne, G. V., Magalhães, A. M., Moffat, A. F., Schulte-Ladbeck, R. E., and Tapia, S., eds., 735–746 (1988).

[4] Dhillon, V. S., Marsh, T. R., Stevenson, M. J., et al., "ULTRACAM: an ultrafast, triple-beam CCD camera for high-speed astrophysics," *MNRAS* **378**, 825–840 (2007).

[5] Greiner, J., Bornemann, W., Clemens, C., et al., "GROND: a 7-Channel Imager," *PASP* **120**, 405–424 (2008).

[6] Potter, S., Buckley, D., O'Donoghue, D., et al., "A new two channel high-speed photo-polarimeter (HIPPO) for the SAAO," *Proc SPIE* **7014**, 179 (2008).

[7] Steele, I. A., Bates, S. D., Guidorzi, C., Mottram, C. J., Mundell, C. G., and Smith, R. J., "RINGO2: an EMCCD-based polarimeter for GRB followup," *Proc SPIE* **7735**, 142 (2010).

[8] Roelfsema, R., Schmid, H. M., Pragt, J., et al., "The ZIMPOL high-contrast imaging polarimeter for SPHERE: design, manufacturing, and testing," *Proc. SPIE* **7735**, 144 (2010).

[9] Rodrigues, C. V., Jablonski, F. J., D'Amico, F., Cieslinski, D., Steiner, J. E., Diaz, M. P., and Hickel, G. R., "Optical polarimetry and infrared photometry of two AM Her binaries: 1RXS J161008.0+035222 and 1RXS J231603.9-052713," *MNRAS* **369**, 1972–1982 (2006).

[10] Costa, J. E. R. and Rodrigues, C. V., "Stokes imaging of AM Her systems using 3D inhomogeneous models - I. Description of the code and an application to V834 Cen," *MNRAS* **398**, 240–248 (2009).

[11] Jablonski, F. J., Pereira, M. G., Braga, J., and Gneiding, C. D., "Discovery of Optical Pulsations in V2116 Ophiuchi equivalent to GX 1+4," *ApJ* **482**, L171 (1997).

[12] Kanaan, A., Nitta, A., Winget, D. E., et al., "Whole Earth Telescope observations of BPM 37093: A seismological test of crystallization theory in white dwarfs," *A&A* **432**, 219–224 (2005).
[13] Kepler, S. O., Nather, R. E., Winget, D. E., et al., "The everchanging pulsating white dwarf GD358," *A&A* **401**, 639–654 (2003).
[14] Carciofi, A. C. and Magalhães, A. M., "The Polarization Signature of Extrasolar Planet Transiting Cool Dwarfs," *ApJ* **635**, 570–577 (2005).
[15] Martioli, E., [*Characterization of exoplanet candidates from Hubble Space Telescope astrometry, ground-based radial velocity, and infrared interferometry*], PhD Thesis, INPE, Brazil (2010).
[16] Tusnski, L. R. M. and Valio, A., "Transit Model of Planets with Moon and Ring Systems," *ApJ* **743**, 97 (2011).
[17] Hayek, W., Sing, D., Pont, F., and Asplund, M., "Limb darkening laws for two exoplanet host stars derived from 3D stellar model atmospheres. Comparison with 1D models and HST light curve observations," *A&A* **539**, A102 (2012).
[18] Howarth, I. D., "On stellar limb darkening and exoplanetary transits," *MNRAS* **418**, 1165–1175 (2011).
[19] Choi, J.-Y., Shin, I.-G., Park, S.-Y., et al., "Characterizing Lenses and Lensed Stars of High-magnification Single-lens Gravitational Microlensing Events with Lenses Passing over Source Stars," *ApJ* **751**, 41 (2012).
[20] Batista, V., Gould, A., Dieters, S., et al., "MOA-2009-BLG-387Lb: a massive planet orbiting an M dwarf," *A&A* **529**, A102 (2011).
[21] Gould, A., Dong, S., Gaudi, B. S., et al., "Frequency of Solar-like Systems and of Ice and Gas Giants Beyond the Snow Line from High-magnification Microlensing Events in 2005-2008," *ApJ* **720**, 1073–1089 (2010).
[22] Sumi, T., Bennett, D. P., Bond, I. A., et al., "A Cold Neptune-Mass Planet OGLE-2007-BLG-368Lb: Cold Neptunes Are Common," *ApJ* **710**, 1641–1653 (2010).
[23] Rodrigues, C. V., Jablonski, F. J., Gregorio-Hetem, J., Hickel, G. R., and Sartori, M. J., "Optical Polarization and Near-Infrared Photometry of the Proto-planetary Nebula Henize 3-1475," *ApJ* **587**, 312–319 (2003).
[24] Pereyra, A., Girart, J. M., Magalhães, A. M., Rodrigues, C. V., and de Araújo, F. X., "Near infrared polarimetry of a sample of YSOs," *A&A* **501**, 595–607 (2009).
[25] Pereyra, A., Rodrigues, C. V., and Magalhães, A. M., "Polarimetry of the binary PDS 144," *A&A* **538**, A59 (2012).
[26] Carciofi, A. C., Magalhães, A. M., Leister, N. V., Bjorkman, J. E., and Levenhagen, R. S., "Achernar: Rapid Polarization Variability as Evidence of Photospheric and Circumstellar Activity," *ApJ* **671**, L49–L52 (2007).
[27] Mouschovias, T. C. and Ciolek, G. E., "Magnetic Fields and Star Formation: A Theory Reaching Adulthood," in [*NATO ASIC Proc. 540: The Origin of Stars and Planetary Systems*], Lada, C. J. and Kylafis, N. D., eds., 305 (1999).
[28] McKee, C. F. and Ostriker, E. C., "Theory of Star Formation," *ARAA* **45**, 565–687 (2007).
[29] Pereyra, A. and Magalhães, A. M., "Polarimetry toward the IRAS Vela Shell. I. The Catalog," *ApJSS* **141**, 469–483 (2002).
[30] Pereyra, A. and Magalhães, A. M., "Polarimetry toward the Musca Dark Cloud. I. The Catalog," *ApJ* **603**, 584–594 (2004).
[31] Pereyra, A. and Magalhães, A. M., "Polarimetry toward the IRAS Vela Shell. II. Extinction and Magnetic Fields," *ApJ* **662**, 1014–1023 (2007).
[32] Alves, F. O., Franco, G. A. P., and Girart, J. M., "Optical polarimetry toward the Pipe nebula: revealing the importance of the magnetic field," *A&A* **486**, L13–L16 (2008).
[33] Franco, G. A. P., Alves, F. O., and Girart, J. M., "Detailed Interstellar Polarimetric Properties of the Pipe Nebula at Core Scales," *ApJ* **723**, 146–165 (2010).
[34] Rodrigues, C. V., Sartori, M. J., Gregorio-Hetem, J., and Magalhães, A. M., "The Alignment of the Polarization of Herbig Ae/Be Stars with the Interstellar Magnetic Field," *ApJ* **698**, 2031–2035 (2009).
[35] Targon, C. G., Rodrigues, C. V., Cerqueira, A. H., and Hickel, G. R., "Correlating the Interstellar Magnetic Field with Protostellar Jets and Its Sources," *ApJ* **743**, 54 (2011).

[36] Rodrigues, C. V., Magalhães, A. M., Coyne, G. V., and Piirola, V., "Dust in the Small Magellanic Cloud: Interstellar Polarization and Extinction," *ApJ* **485**, 618 (1997).

[37] Dominici, T. P., Abraham, Z., and Galo, A. L., "Optical and near-infrared simultaneous observations of the BL Lacs PKS 2005-489 and PKS 2155-304," *A&A* **460**, 665–672 (2006).

[38] Dominici, T., Abraham, Z., Pereyra, A., and Magalhães, A. M., "Optical polarization variability in TeV blazars," in [*Blazar Variability across the Electromagnetic Spectrum*], (2008).

[39] Barres de Almeida, U., Ward, M. J., Dominici, T. P., et al., "Particle acceleration and magnetic field structure in PKS2155-304: optical polarimetric observations," *MNRAS* **408**, 1778–1787 (2010).

[40] Sicardy, B., Ortiz, J. L., Assafin, M., et al., "A Pluto-like radius and a high albedo for the dwarf planet Eris from an occultation," *Nature* **478**, 493–496 (2011).

[41] Assafin, M., Campos, R. P., Vieira Martins, R., da Silva Neto, D. N., Camargo, J. I. B., and Andrei, A. H., "Instrumental and digital coronagraphy for the observation of the Uranus satellites upcoming mutual events," *Planet. Space Sci.* **56**, 1882–1887 (2008).

[42] Assafin, M., Vieira-Martins, R., Braga-Ribas, F., Camargo, J. I. B., da Silva Neto, D. N., and Andrei, A. H., "Observations and Analysis of Mutual Events between the Uranus Main Satellites," *AJ* **137**, 4046–4053 (2009).

[43] Assafin, M., Camargo, J. I. B., Vieira Martins, R., et al., "Precise predictions of stellar occultations by Pluto, Charon, Nix, and Hydra for 2008-2015," *A&A* **515**, A32 (2010).

[44] Lee, Y. S., Beers, T. C., Sivarani, T., et al., "The SEGUE Stellar Parameter Pipeline. I. Description and Comparison of Individual Methods," *AJ* **136**, 2022–2049 (2008).

[45] Yanny, B., Rockosi, C., Newberg, H. J., et al., "SEGUE: A Spectroscopic Survey of 240,000 Stars with g = 14-20," *AJ* **137**, 4377–4399 (2009).

[46] Allende Prieto, C., Beers, T. C., Wilhelm, R., Newberg, H. J., Rockosi, C. M., Yanny, B., and Lee, Y. S., "A Spectroscopic Study of the Ancient Milky Way: F- and G-Type Stars in the Third Data Release of the Sloan Digital Sky Survey," *ApJ* **636**, 804–820 (2006).

[47] Magalhães, A. M., Pereyra, A., Melgarejo, R., et al., "A Southern Optical/Infrared Survey of Interstellar Polarization," in [*Astronomical Polarimetry: Current Status and Future Directions*], Adamson, A., Aspin, C., Davis, C., and Fujiyoshi, T., eds., *ASPCS* **343**, 305 (2005).

[48] Fukugita, M., Ichikawa, T., Gunn, J. E., Doi, M., Shimasaku, K., and Schneider, D. P., "The Sloan Digital Sky Survey Photometric System," *AJ* **111**, 1748 (1996).

[49] Gunn, J. E. and Stryker, L. L., "Stellar spectrophotometric atlas, wavelengths from 3130 to 10800 A," *ApJS* **52**, 121–153 (1983).